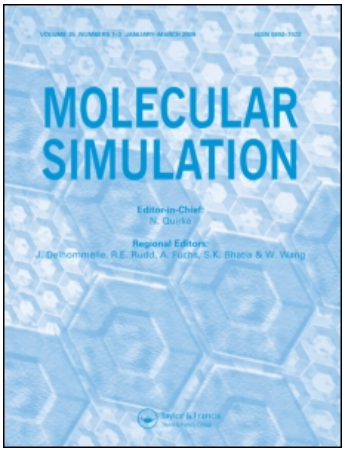

Molecular Simulation
Publication details, including instructions for authors and subscription information:
http://www.informaworld.com/smpp/title~content=t713644482

Design, docking studies and molecular dynamics of new potential selective inhibitors of *Plasmodium falciparum* serine hydroxymethyltransferase

Manuela Leal da Silva[a]; Arlan da Silva Gonçalves[b]; Paulo Ricardo Batista[b]; José Daniel Figueroa-Villar[a]; Pedro Geraldo Pascutti[b]; Tanos Celmar Costa França[a]
[a] Divisão de Ensino e Pesquisa, Seção de Engenharia Química, Instituto Militar de Engenharia, Rio de Janeiro, CEP, Brazil [b] Instituto de Biofísica Carlos Chagas Filho, CCS, Rio de Janeiro, UFRJ, CEP, Brazil

First published on: 28 July 2009

To cite this Article da Silva, Manuela Leal , da Silva Gonçalves, Arlan , Ricardo Batista, Paulo , Figueroa-Villar, José Daniel , Pascutti, Pedro Geraldo and França, Tanos Celmar Costa(2010) 'Design, docking studies and molecular dynamics of new potential selective inhibitors of *Plasmodium falciparum* serine hydroxymethyltransferase', Molecular Simulation, 36: 1, 5 — 14, First published on: 28 July 2009 (iFirst)
To link to this Article: DOI: 10.1080/08927020903051580
URL: http://dx.doi.org/10.1080/08927020903051580

Molecular Simulation
Vol. 36, No. 1, January 2010, 5–14

Taylor & Francis
Taylor & Francis Group

Design, docking studies and molecular dynamics of new potential selective inhibitors of *Plasmodium falciparum* serine hydroxymethyltransferase

Manuela Leal da Silva[a], Arlan da Silva Gonçalves[b], Paulo Ricardo Batista[b], José Daniel Figueroa-Villar[a], Pedro Geraldo Pascutti[b] and Tanos Celmar Costa França[a]*

[a]*Divisão de Ensino e Pesquisa, Seção de Engenharia Química, Instituto Militar de Engenharia, Praça General Tibúrcio 80, CEP 22290-270, Rio de Janeiro, Brazil;* [b]*Instituto de Biofísica Carlos Chagas Filho, CCS, Avenida Carlos Chagas Filho, 373, Edifício do CCS, Bloco D, Sala D1-030, Ilha do Fundão, UFRJ, CEP 21941-902, Rio de Janeiro, Brazil*

(*Received 8 February 2009; final version received 12 May 2009*)

In this paper, former studies on the interactions of the natural substrate and potential inhibitors of *Plasmodium falciparum* serine hydroxymethyltransferase (*Pf*SHMT) were used to design five new potential selective inhibitors to this enzyme. Results of the docking energies calculations of these structures inside the active sites of *Pf*SHMT and human SHMT were used to select a more suitable structure as a potential selective inhibitor to *Pf*SHMT. Further molecular dynamics studies of this molecule and 5-formyl-6-hydrofolic acid (natural substrate) docked inside these enzymes' active sites revealed important features for additional refinements of this structure and also additional residues in the *Pf*SHMT active site to be considered further for designing selective inhibitors.

Keywords: malaria; *Pf*SHMT; docking; molecular dynamics; selective inhibitors

1. Introduction

According to the World Health Organization, malaria is by far the tropical disease causing most of the social and economic problems in the world today, being passed in the number of deaths only by AIDS [1].

Also known as paludisme, malaria is a public health problem in more than 90 countries, where about 2.4 billion people are under the risk of contamination [2]. This disease affects about 300–500 million people annually causing about 2.5 million deaths, mostly among children. Today the threat is worst in Latin American countries, African countries and in vast areas of the Meridian, Asia and Oceania [3,4]. This means that 40% of the world's population is at risk of developing malaria [3,5].

In Brazil, malaria is concentrated in the Amazonian region with more than 99% of registered cases in the country. In other states, the registered cases are almost totally imported from the Amazonian region or other countries where the transmission also occurs [1].

Two aspects that have currently stimulated new efforts regarding the development of chemotherapy, vaccines and sanitary studies about malaria are: the rapid emergence of *Plasmodium falciparum* strains that are resistant to currently available antimalarial drugs [6–9] and the inefficacy of antimalarial vaccines [3]. Since a vaccine for malaria seems to be far in the future, a more immediate solution would be the development of new anti-malarial chemotherapy. Still, we have to assume that the ability of *Plasmodium* to adapt to new chemotherapy under the pressure of the drugs would eventually render any new antimalarial drug less efficient, thus making all research on the aspects of malaria even more important. Many strategies have been adopted to develop new drugs for malaria. Among them, we have been interested in the design of new inhibitors for the three enzymes involved in the parasite methylenetetrahydrofolate cycle using molecular modelling and dynamics studies, and have already performed several studies focussed on the design of new potential inhibitors for the enzymes dihydrofolate reductase–thymidylate synthase (DHFR-TS) and serine hydroxymethyltransferase (SHMT) from *P. falciparum* [10–13].

In a former work the first multiple-alignment homology model of dimmeric *P. falciparum* SHMT (*Pf*SHMT) was proposed with the coenzyme piridoxal 5′-fosfato bound to glycine (PLG) and its natural substrate, 5-formyl-6-hydrofolic acid (FFO), and anchored into its active sites [12]. This model was further used to build seven holoenzymes docked with FFO analogues designed according to the differences observed in the behaviour of the FFO tail along molecular dynamics (MD) simulations, in the active sites of *Pf*SHMT and human SHMT (*Hs*SHMT) [13]. Further MD simulations and interaction energy estimations of the compounds positioned in the active sites of both enzymes showed that compounds with a negative net charge and possessing either shorter tails or longer amphoteric tails would be more selective towards *Pf*SHMT [13]. Based on this information, we designed, in this work, five new potential selective inhibitors to

*Corresponding author. Email: tanos@ime.eb.br

ISSN 0892-7022 print/ISSN 1029-0435 online

DOI: 10.1080/08927020903051580
http://www.informaworld.com

*Pf*SHMT and calculated their docking energies inside the active sites of *Hs*SHMT and *Pf*SHMT. From the data obtained, the more suitable structure as a potential selective inhibitor to *Pf*SHMT was selected. Further MD studies of this molecule and PLG docked inside the active sites of both enzymes revealed important insights for additional refinements that were needed on this structure in order to increase its efficiency as a potential *Pf*SHMT selective inhibitor and, also, additional residues in the *Pf*SHMT active site to be considered further for designing selective inhibitors.

2. Methodology

2.1 Docking studies

The structures of PLG, FFO and the five compounds to be studied as potential *Pf*SHMT inhibitors were first built using the Gaussian View software from the Gaussian 98 package® [14]. After that, the molecules had their atomic partial charges calculated at the Hartree-Fock level with the 6-31G* basis set using the CHELPG approach of the Gaussian 98 package® [14] and their topological files generated at the Dundee PRODRG server [15].

The calculation of the docking energies of FFO and the five new compounds inside the active sites of *Pf*SHMT and *Hs*SHMT was performed using the software, AutoDock-Tools and AutoDdock 3.0.5 [16]. The input files of the ligands in the format suitable for AutoDock 3.0.5 [16] (.pdbq) were generated at the Dundee PRODRG server [15]. The input files of *Pf*SHMT and *Hs*SHMT used for the docking calculations were the output files after the 1000 ps of MD simulations reported by França et al. [12].

The grid sizes used for the dockings inside the enzymes' active sites were defined as 60 × 70 × 60 Å for both the enzymes with 0.375 Å as space between the grid points or about a quarter of a C—C bond. As a parameter for the molecular docking, the Lamarckian genetic algorithm [16], a combination between the Genetic algorithm and the Local Search Pseudo-Solis and Wets algorithm, was employed [16]. The number of predicted conformations for the simulations was 100 and the maximum number of generations performed by the genetic algorithm was 27,000. The 100 lowest-energy conformations were selected by the software as the best ligand conformations in the receptor site.

2.2 Molecular simulations studies

The insertions of the proposed inhibitor, FFO and PLG into the *Pf*SHMT and *Hs*SHMT active sites for the MD simulations were performed by superposition of FFO and PLG in the same conformations as present in the 3D structure of *Pf*SHMT reported by França et al. [12] and the *Hs*SHMT 3D structure used for this task was the one reported by Renwick et al. [17] (PDB entry 1BJ4, resolution = 2.65 Å, *R*-value = 0.210).

The MD steps were carried out according to the following procedure: first, a 50 ps of MD at 300 K in the water molecules inside the box in order to allow for the equilibration of the solvent around the protein residues. In this simulation, all protein atoms had their positions restrained. Then, a full MD simulation of 3000 ps at 300 K with no restrictions was carried out, using 1 fs of integration time and a cut-off of 14 Å for long-range interactions.

Because these proteins have only a residual net charge, which was balanced by counter-ions for these simulations, it was possible to use the direct cut-off for long-range interactions without smoothening functions. The effects of the electrostatic potential truncation are minor at 14 Å, and the cut-off procedure makes the calculations faster than the other methods. Considering that the protein and the water molecules inside the simulation box are composed of about 100,000 atoms, this method can save significant computational time.

As a whole, 3000 conformations were stored during each simulation. In this step the pair lists were updated for every 500 time steps and all the Lys and Arg residues were positively charged while the Glu and Asp residues were negatively charged.

Also, in order to obtain a neutral net charge for all the systems, the charges were neutralised by the addition of Na^+ ions. The programme calculates the electrostatic potential to find the best positions for ion insertion by replacing water molecules that are at least at 3.50 Å from the protein surface. Periodic boundary conditions were employed and the water model used was the single point charge water, the default solvent of the GROMACS 3.2 package [18,19].

3. Results and discussion

3.1 Proposition of potential selective inhibitors for PfSHMT

The first step of this work consisted of simplifying the structures of the potential *Pf*SHMT inhibitors formerly proposed by França et al. [13] (Figure 1) in order to propose simpler structures from a synthetic point of view and, also, to try to correlate the features of those structures with the known antimalarial drugs. The studies performed by França et al. [13] showed that, to act as selective ligands for the *Pf*SHMT active site, the tails of the FFO analogues should be short, in order to avoid the repulsive interactions with residues Lys138, Lys139 and Lys140 of the active site of *Pf*SHMT, as is the case for compounds **3** and **7** in Figure 1. On the other hand, the tails may also be longer, but in this case they must possess both negative and positive charges at specific positions in order to explore their interactions with Lys138, Lys139, Lys140 and Glu137.

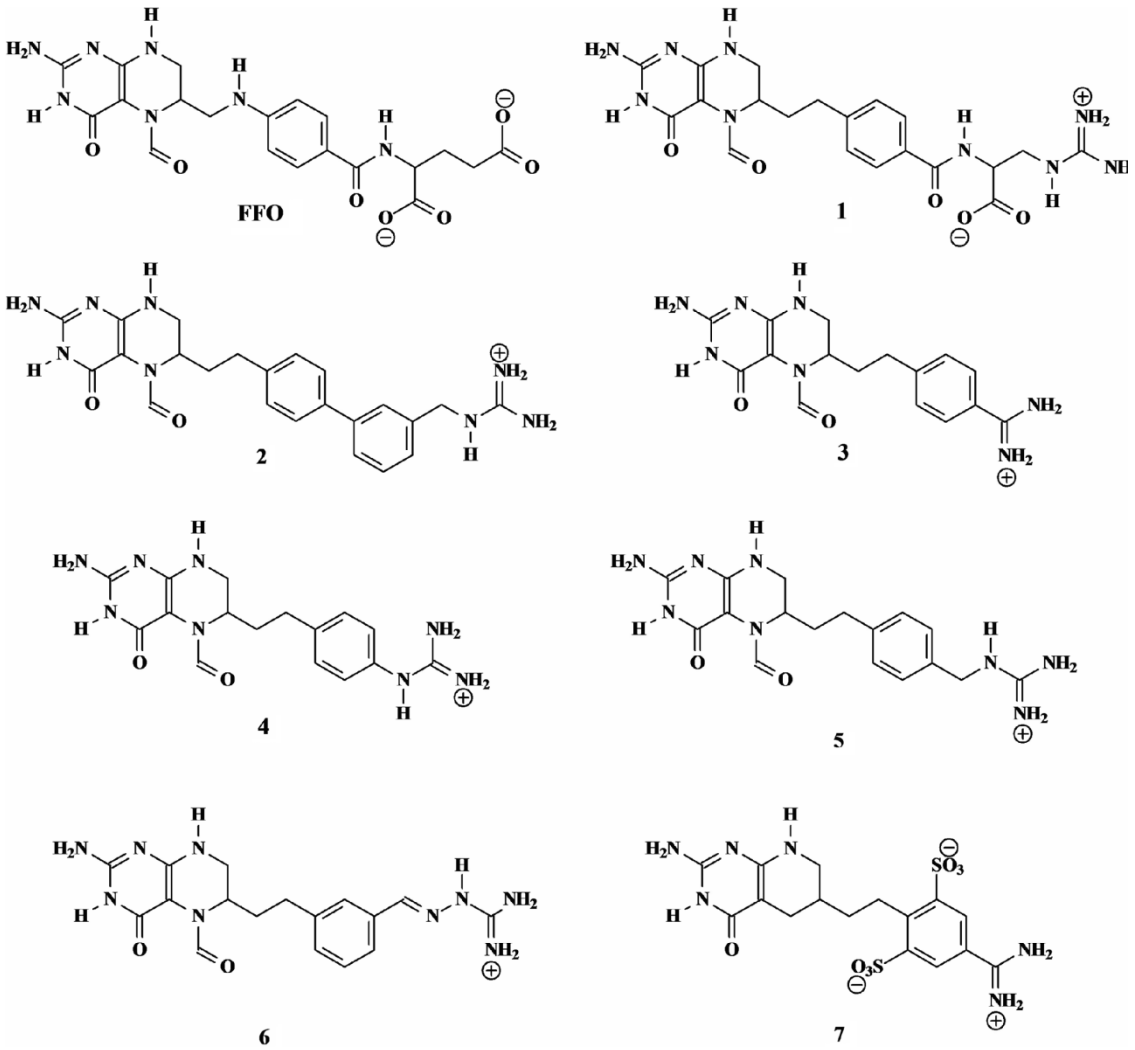

Figure 1. Structures of FFO and the seven compounds proposed by França et al. [13].

Figure 2 shows the structures of the five compounds proposed in this work. Compounds **1** and **2** are two additional derivatives of folate similar to the compounds already studied by França et al. [13] and presented in Figure 1. Compounds **3**–**5**, on the other hand, are derivatives of trimetopima, a known antimalarial drug belonging to the class of the 2,4-diaminopyrimidines. The study of these compounds, besides giving continuity to the studies started by França et al. [13], also makes a correlation of the features suggested in that work, to improve the drug affinities to our target (SHMT), with the structures of a class of antimalarial drugs, already commercially available, in order to propose new structures of derivatives of those drugs that could be even more active. Another important contribution is the fact that literature describes 2,4-diaminopirimidines as specific DHFR inhibitors [20–22]. The proposition of molecules of this class, also able to target SHMT, could afford new antifolates that are eventually more efficient in the fight against resistance, once SHMT is an enzyme less susceptible to mutation [12,13].

In compounds **1** and **2**, the pteridinic ring was replaced by a pyrimidinic one and the only modification on the *para*-amino benzoic acid (PABA) portion of these molecules related to FFO was the replacement of the N atom in the bridge linking the PABA portion to the pteridinic ring by an O atom, in compound **1**, and by changing the positions of the N and C atoms in the same bridge in compound **2**. These modifications had the goal of avoiding the ligand acting as an enzyme agonist once that N atom in FFO participates in the mechanism of action of SHMT by forming an aldimine [23].

In compounds **3**–**5** the FFO pteridinic ring was replaced by a 2,4,6-triamino-pyrimidinic ring in order to afford the trimetoprime derivatives already mentioned above. In the same way as for compounds **1** and **2**, the N atom in the bridge linking the rings was substituted to avoid agonism. The tails of all compounds are positives

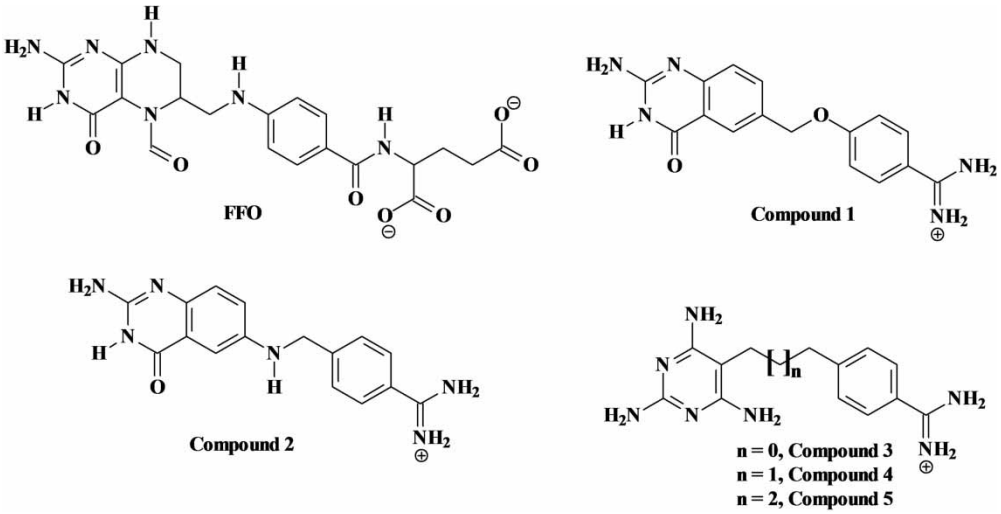

Figure 2. Structures of FFO and compounds **1**–**5**.

with a diamine substituent in order to potentialise interactions with Glu137 in *Pf*SHMT.

In compounds **3**–**5** we also modified the size of the linking bridge in order to verify how the tail length would influence the interaction with the active sites in both enzymes and define the ideal length to maximise interactions with the active-site residues.

As already mentioned, all modifications had the goal of facilitating the synthetic process and preserving the features considered important to a selective inhibitor of *Pf*SHMT. Figure 3 illustrates this by showing proposals of generic synthetic routes for compounds **1**–**5**.

The hypotheses that such compounds could also interact with the other enzymes of the folate cycle provoking a collateral and toxic effect to the human host is not forgotten. Metabolic and toxicological studies, however, are part of a step subsequent to finding a prototype in the drug design [24]. Our proposal in this work was just to propose structures with potentially more affinity by *Pf*SHMT taking into account a feasible synthetic route.

3.2 Docking studies of the proposed inhibitors

After optimisation and generation of the .pdbq files in the PRODRG Dundee server [15], FFO and compounds **1**–**5** were docked, using the software AutoDock 3.0.5 [16], inside the active sites of *Pf*SHMT and *Hs*SHMT, already anchored with PLG, in order to compare their docking energies and also to estimate their selectivity related to *Hs*SHMT. This same computational procedure has been already employed in literature for similar systems, with good results [25,26].

For the docking energies calculations we used the .pdbq files of *Pf*SHMT and *Hs*SHMT, anchored with PLG and FFO, generated by França et al. [12] after 1000 ps of MD simulations. The FFO coordinates were removed from each active site in order to liberate space for the docking grid. The docking energies of FFO and compounds **1**–**5** were calculated according to the procedure described in the methodology section and the best 100 conformations generated for each compound, inside each active site, by the final docking energies (FDE) were analysed. The FDE are calculated by adding the final intermolecular energies (FIE) to the final internal energy of ligand (FIEL).

Table 1 presents the values of the lowest docked energies (LDE) among the 100 conformations and the mean docked energies (MDE) among the values of FDE for each molecule in *Pf*SHMT and *Hs*SHMT active sites, respectively. Besides, Table 1 also presents the Boltzmann relationship [27,28] for each ligand in *Pf*SHMT and *Hs*SHMT. Boltzmann launched the basis of the statistical mechanics by introducing statistics in the explanation of the natural phenomena [28–30]. One of the Boltzmann relationships [Equation (1)] helps us to create a relationship between two populations when analyzing their energy levels

$$\frac{N_2}{N_1} = \mathrm{e}^{-\Delta E/kT}. \tag{1}$$

In Equation (1), ΔE is the energy variation for each system, k is the Boltzmann constant ($1.38 \times 10^{-23}\,\mathrm{J\,K^{-1}}$) and T is the system temperature in Kelvin degrees. In this relationship if, by any way, we increase the concentration of one of the populations, the concentration of the other will be reduced. The bigger the relationship N_2/N_1, bigger would be the affinity for one enzyme related to another.

The Boltzmann relationships for each ligand in *Pf*SHMT and *Hs*SHMT were calculated from the MDE

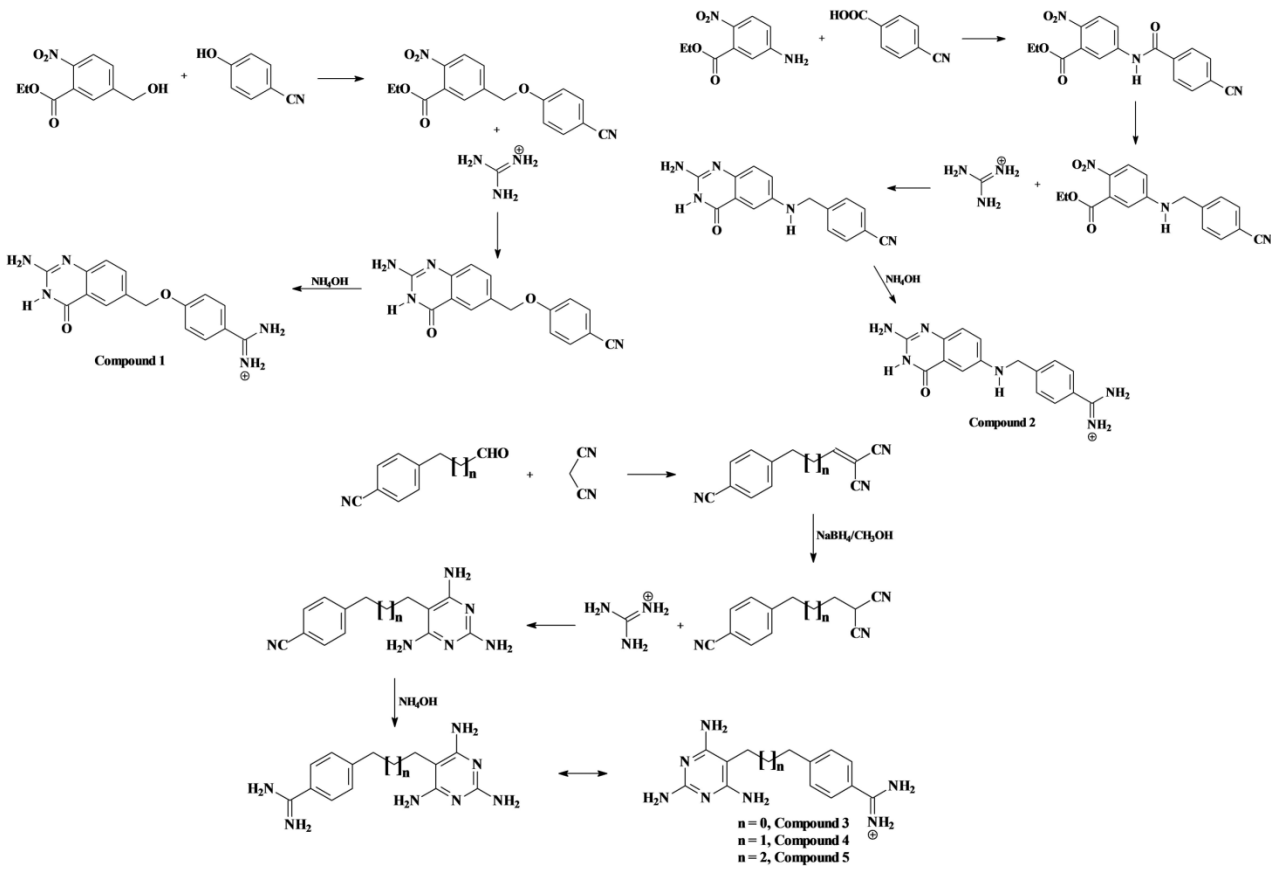

Figure 3. Possible synthetic routes for compounds **1**–**5**.

Table 1. LDE, MDE (kcal mol^{-1}) and Boltzmann relationship for the ligands docked in *Hs*SHMT and *Pf*SHMT active sites.

	*Hs*SHMT [N_1 (kcal mol^{-1})]		*Pf*SHMT [N_2 (kcal mol^{-1})]		N_2:N_1
Ligand	LDE	MDE	LDE	MDE	$\frac{N_2}{N_1} = e^{-\Delta E/kT}$
FFO	− 16.02	− 12.43	− 14.51	− 12.75	–
Compound **1**	− 12.83	− 11.30	− 11.89	− 10.40	18.03:81.97
Compound **2**	− 13.30	− 11.30	− 12.69	− 11.40	54.07:45.93
Compound **3**	− 11.57	− 10.10	− 11.35	− 9.70	34.25:65.75
Compound **4**	− 10.75	− 9.53	− 11.91	− 11.74	97.35:2.65
Compound **5**	− 9.03	− 7.74	− 10.60	− 8.85	85.93:14.07

at a temperature of 310 K considering *Hs*SHMT as N_1 and *Pf*SHMT as N_2. Table 1 presents the values of the Boltzmann relationships obtained together with the LDE and the MDE for each ligand.

From Table 1 one can see that FFO, as already expected, presents better docking energy (DE) values (more negative) for both enzymes. Besides, the difference observed in the DE values between each compound in the active sites is about 2.0 kcal mol^{-1}, which makes difficult to choose the best compound based only on the DE analysis. On the other hand, using Boltzmann relationships we can have an idea of what those differences mean.

As can be seen by the Boltzmann relationship, compounds **4** and **5** are the only ones that would present bigger populations of molecules inside the *Pf*SHMT active site with 97.35 and 85.95%, respectively. Compounds **1** and **3** would present more affinity for *Hs*SHMT while the molecules of compound **2** would practically be distributed equally between the two enzymes. These preliminary results suggest that compounds **4** and **5** would be potentially more selective to *Pf*SHMT.

Once compound **4** was found to be the most promising according to the Boltzmann relationship calculations [28], we decided to choose it in order to perform an initial qualitative analysis on its possible interactions with the active sites of *Pf*SHMT and *Hs*SHMT by comparing its physiological behaviour with FFO through MD simulations studies.

3.3 MD simulations

In order to perform the MD simulation steps, FFO and compound **4** were docked, together with the PLG, inside the active sites of *Pf*SHMT and *Hs*SHMT, affording four enzyme/PLG/ligand complexes. This docking was accomplished using, as reference, the *Pf*SHMT structure docked with PLG and FFO reported by França et al. [12]. Each complex was submitted to 50 ps of position-restrained MD followed by 3000 ps of MD simulations with no restriction, as described in the methodology section, and following the same technique already employed in the former molecular modelling studies involving the enzymes *Pf*DHFR [11] and *Leishmania donovani* nucleoside hydrolase [31].

Calculations of the temporal root mean square deviation (RMSD) were carried out for all the atoms in all the systems for 500 frames generated at each 2 ps of MD simulation. In this case the result is a unique general value for each enzyme monitored throughout the whole simulation time. Taking into account that the complexes could float inside the water box, each frame was adjusted to the former by the minimum squares method when calculating the SD. In Figure 4, where the variation of the energy with time is monitored for the systems *Hs*SHMT/PLG/FFO and *Pf*SHMT/PLG/FFO, it can be observed that the systems equilibrate along the first 500 ps of the MD simulation. This behaviour was common to all the four MD simulations. We also observed that, for all

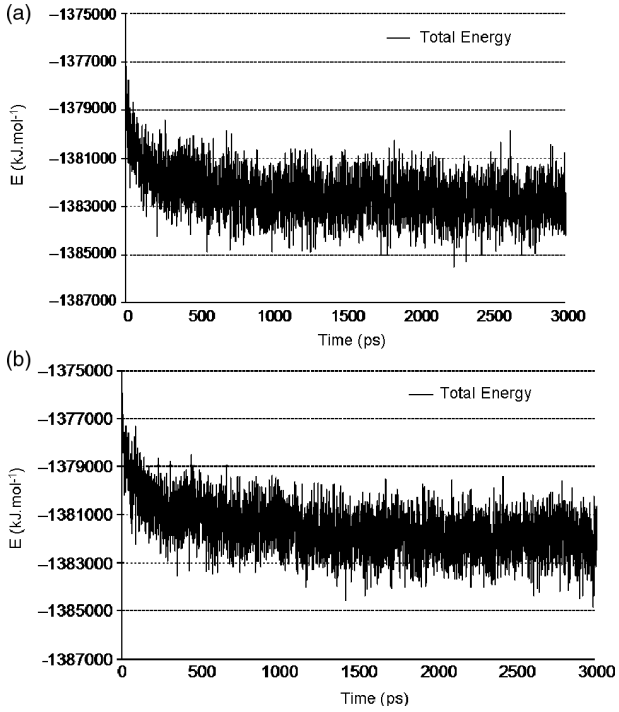

Figure 4. Energy variation along the 3000 ps of MD simulation of: (a) system *Hs*SHMT/PLG/FFO and (b) system *Pf*SHMT/PLG/FFO.

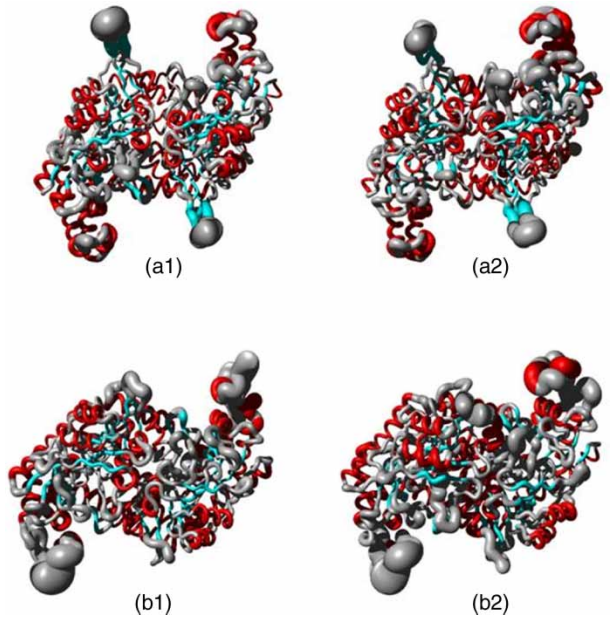

Figure 5. Qualitative illustrations of RMSF for the MD simulations of: (a1) *Hs*SHMT/PLG/FFO; (a2) *Hs*SHMT/PLG/compound **4**; (b1) *Pf*SHMT/PLG/FFO; (b2) *Pf*SHMT/PLG/compound **4**. Red tubes correspond to α-helix; blue tubes correspond to β-sheets and light grey tubes correspond to loops. (Colour available in online version).

simulations, the temporal RMSD of the SHMTs as apoenzymes practically fits the temporal RMSD of the complexes (data not shown). Also, as expected, the ligands display a greater fluctuation than the whole complexes but with a smaller RMSD, thus confirming the stability of the MD simulations.

The spatial RMSD (RMSF) of each amino acid residue was also calculated in the time range of 100–3000 ps, at each ps, totalizing 2900 frames. In Figure 5 are shown the qualitative illustrations in the tube representation of the RMSF for the systems. Analyzing this figure it can be determined that the most mobile regions along the MD simulations are the regions with major thickness of the tubes. These regions correspond to the residues near the two terminuses of each monomer and to the loops regions. On the other hand, the residues at the active site regions, as well as those at the α-helix and β-sheet regions, present lower RMSF values, revealing to be the most stable regions of the system. Along the MD simulations, very few fluctuations exceeded 0.2 nm and even less over passed 0.4 nm.

*3.3.1 Behaviour of FFO and compound **4** along the MD simulations*

In MD simulations it is possible to analyse the atoms' fluctuations inside the enzymes' active sites. The superposition of the ligand structures recorded at each 100 ps of MD simulations affords a visual idea of the stability of each part of the molecule along the simulation.

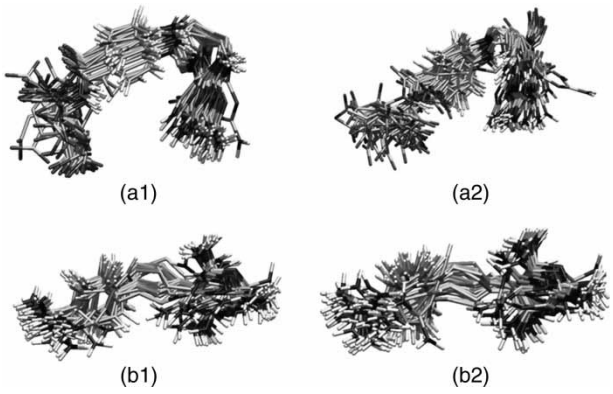

Figure 6. Superposition of the structures of FFO and structures of compound **4** along the MD simulation. (a1) FFO in the system *Hs*SHMT/PLG/FFO; (a2) FFO in the system *Pf*SHMT/PLG/FFO; (b1) compound **4** in the system *Hs*SHMT/PLG/compound **4**; (b2) compound **4** in the system *Pf*SHMT/PLG/compound **4**.

The superposition of the structures of FFO and structures of compound **4** obtained along all the simulation are shown in Figure 6, where one can see that both the ligands stabilise well in both systems with major fluctuations occurring only in their extremities.

3.3.2 Analysis of the hydrogen bonds (HBs) along the MD simulation

Non-covalent interactions are essential for the maintenance of the protein structure, for recognising processes and for the enzyme–ligand interactions. The HB is a special kind of interaction between non-bonded atoms with a very important role in the affinity of a molecule for an enzyme. In this work we investigated only the HBs formed and maintained between each enzyme and each ligand. These HBs were classified as direct HBs (dHB) and water intermediated HBs (wHB). In order to evaluate qualitatively the nature of each HB, we calculated the prevalence (temporal occurrence) of each interaction along the 3000 ps of MD simulation for the systems SHMT/PLG/FFO and SHMT/PLG/compound **4**. The results obtained are presented in Tables 2 and 3. These tables report only those HBs with more than 10% of prevalence.

From Table 2 one can see the existence of 10 HBs in the system *Hs*SHMT/PLG/FFO versus 08 HBs in the system *Hs*SHMT/PLG/compound **4**. Besides, there exists only one important wHB (FFO with Asn375) that occurred in 45.2% of the simulation time. This result suggests a better affinity of FFO for *Hs*SHMT.

For the system *Pf*SHMT/PLG/FFO, one can observe the existence of 11 dHBs versus 13, when compared to the system *Pf*SHMT/PLG/compound **4**, plus some additional wHBs (Table 3). Also, for *Pf*SHMT/PLG/FFO there is a HB between Hys129 and FFO occurring in 46.4% of the simulation time and 03 wHBs between Lys237 and FFO. For the system *Pf*SHMT/PLG/compound **4** few wHBs were observed while some dHB remained for more than 20% of the simulation time. Those results suggest a slight preference of compound **4** for the *Pf*SHMT active site.

Table 2. Prevalence of HBs of *Hs*SHMT with FFO and compound **4**.

		*Hs*SHMT/ FFO		*Hs*SHMT/ compound **4**	
Donor	Receptor	dHB	wHD	wHB	wHD
Leu139	FFO	29.9	–	–	–
Asn375	FFO	0.2	45.2	–	–
Asn375	FFO	27.2	0.5	–	–
Lys376	FFO	22.6	3.7	–	–
Thr378	Compound **4**	–	–	15.7	–
Thr378	Compound **4**	–	–	19.0	0.2
Arg392	FFO	13.1	0.1	–	–
Tyr57	FFO	16.4	0.1	–	–
Tyr57	FFO	13.3	0.5	–	–
Compound **4**	Thr378	–	–	15.3	–
Compound **4**	Thr378	–	–	10.5	–
Compound **4**	Thr378	–	–	14.1	0.1
FFO	Tyr62	19.1	2.1	–	–
Compound **4**	Tyr543	–	–	3.5	14.9
Compound **4**	Gln281	–	–	9.1	3.4
Compound **4**	Gly283	–	–	10.2	–
FFO	Gly137	66.7	–	–	–
FFO	Leu139	25.8	–	–	–

Table 3. Prevalence of HBs of *Pf*SHMT with FFO and compound **4**.

		*Pf*SHMT/ FFO		*Pf*SHMT/ compound **4**	
Donor	Receptor	dHB	wHD	dHB	wHD
Leu130	FFO	13.0	–	–	–
Lys237	FFO	3.4	19.5	–	–
Lys237	FFO	2.8	12.6	–	–
Lys237	FFO	3.2	16.0	–	–
Asn354	Compound **4**	–	–	13.5	–
Asn354	Compound **4**	–	–	20.0	–
Asn354	Compound **4**	–	–	22.9	–
Asn354	Compound **4**	–	–	15.2	–
Arg371	FFO	15.2	5.9	–	–
Arg371	Compound **4**	–	–	10.7	–
Arg371	Compound **4**	–	–	16.7	–
FFO	Gly128	14.9	0.1	–	–
FFO	Hys129	12.5	0.2	–	–
INB4	Lys139	–	–	19.1	–
Compound **4**	Lys139	–	–	17.4	0.7
FFO	Ser142	37.6	–	–	–
Compound **4**	Asn354	–	–	23.6	–
Compound **4**	Tyr63	–	–	11.8	–
Compound **4**	Hys129	–	–	11.1	4.3
Compound **4**	Asn354	–	–	24.3	–
Compound **4**	Tyr63	–	–	12.2	0.1
FFO	Thr357	5.3	10.2	–	–
FFO	Arg371	18.0	–	–	–
FFO	Hys129	46.4	4.5	–	–

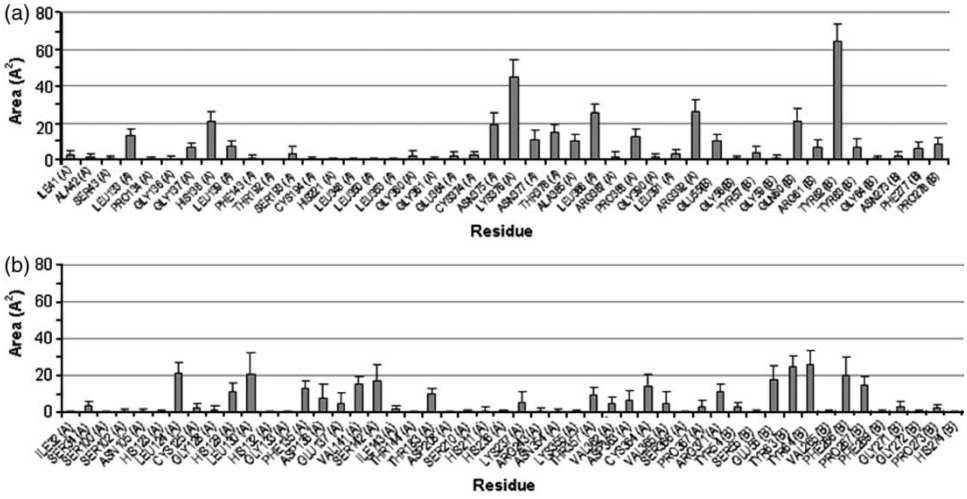

Figure 7. Residues implicated in the surface of intermolecular contact between: (a) *Hs*SHMT and FFO; (b) *Pf*SHMT and FFO. The parenthesis after each residue indicates the chain to which the residue belongs.

3.4 Analysis of the surfaces of intermolecular contact

In order to provide a better understanding of the ligand–enzyme interactions, the surfaces of intermolecular contact of each enzyme with FFO and compound **4** were calculated, discriminated by each residue present in the interfaces SHMT/FFO and SHMT/compound **4**. In this way, it is possible to verify standards of interaction and identify the residues evolved in this interface as well as the residues forming HBs with the ligand.

Analysis of Figures 7 and 8(a) reveals the residues responsible for the intermolecular surface areas in each active site for the systems *Hs*SHMT/ligand. One can notice that the interaction areas for several residues stay above 10 Å^2 suggesting a good interaction of FFO with the enzymes, as already expected. Table 4 present the residues responsible for the surface of intermolecular contact for both enzymes.

In the same way as for *Hs*SHMT, Figures 7 and 8(b) reveal the residues responsible by the intermolecular surface areas in each active site for the systems *Pf*SHMT/ligand. We can see that the areas of interaction for several residues stay above 6 Å^2 suggesting a good interaction of each enzyme with compound **4**. Also, Table 4 presents the residues responsible for the surface of intermolecular contact around compound **4** for both enzymes. As the active sites of dimmeric SHMTs are shared by residues of both the monomers [12], Figures 7 and 8 indicate to which chain each residue belongs.

Comparisons of the interaction surfaces also reveal little differences in the affinity of compound **4** for

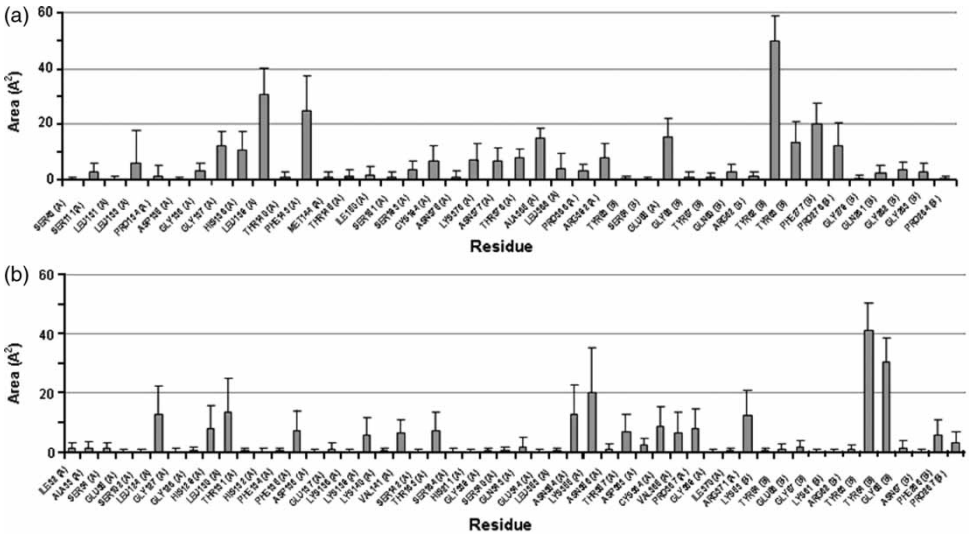

Figure 8. Residues implicated in the surface of intermolecular contact between: (a) *Hs*SHMT and compound **4**; (b) *Pf*SHMT and compound **4**. The parenthesis after each residue indicates the chain to which the residue belongs.

Table 4. Main residues responsible for the surface of contact of SHMT/ligand.

*Hs*SHMT/ FFO	*Pf*SHMT/ FFO	*Hs*SHMT/ compound **4**	*Pf*SHMT/ compound **4**
Glu55	Glu56	Glu93	Tyr63
Gln60	Tyr63	Tyr100	Tyr64
Tyr62	Tyr64	Tyr101	Leu124
Leu133	Leu124	Leu133	Hys129
Gly137	Hys129	Gly137	Leu130
Hys138	Leu130	Hys138	Phe135
Leu139	Phe135	Leu139	Lys139
Pro278	Asp136	Phe143	Val141
Asn375	Val141	Cys194	Thr183
Lys376	Ser142	Phe315	Asn354
Asn377	Thr183	Pro316	Lys355
Thr378	Phe266	Lys376	Thr357
Ala385	Pro267	Asn377	Cys364
Leu386	Thr357	Thr378	Val365
Pro388	Cys364	Ala385	Pro367
Arg392	Arg371	Arg392	Arg371

*Pf*SHMT and *Hs*SHMT. In Tables 2 and 3 we can see the dHBs formed along the MD simulations between the main residues of the contact surface and compound **4**. In this way one can notice that *Hs*SHMT formed dHBs only between residue Thr378 and compound **4** while in *Pf*SHMT compound **4** formed dHBs with the residues Tyr63, Hys129, Lys139, Asn354 and Arg371.

Another important achievement of the analysis of the surfaces of intermolecular contacts is the fact that it was possible to observe some important residues in the enzymes, interaction sites not reported earlier by França et al. [12]. For *Hs*SHMT we observed the residues Pro278, Lys376 and Ala385 interacting with FFO as well as with compound **4** and for *Pf*SHMT there were observed the residues Phe135, Val141, Thr357 and Cys364. This information could be very useful for additional studies of selective inhibitors to *Pf*SHMT.

4. Conclusion

In the first step of this work, we performed docking studies of five potential *Pf*SHMT selective inhibitors conceived and designed from the insights into selective inhibition of *Pf*SHMT reported by França et al. [12] and having in mind the correlation to structures of a known antifolate besides the proposition of simpler structures from a synthetic point of view. Docking results suggested that the fused rings on the pteridinic portion of FFO could not be an essential feature for a good interaction of the ligands with the *Pf*SHMT active site and, also, that the tail size could be an important factor to be considered, once the more flexible and big-tailed compounds **4** and **5** were more selective related to the more rigid compounds **1** and **2** and the short-tailed compound **3**. These results also suggest that the derivatives of DHFR inhibitors such as compounds **4** and **5** could also be potential SHMT inhibitors affording new antifolates eventually more efficient in the fight against resistance, if we take into account that SHMT is an enzyme less susceptible to mutation [12,13].

In the second step we performed 3000 ps of MD simulations of compound **4** and FFO anchored in the active sites of *Pf*SHMT and *Hs*SHMT in order to make a qualitative investigation of its interactions with the *Pf*SHMT and *Hs*SHMT active sites. The analysis of the dynamic behaviour of FFO and compound **4** along the MD simulations allied to the HB analysis suggested the following. (1) Compound **4**, despite stabilising well inside both active sites, forms and maintains more HBs with *Pf*SHMT than with *Hs*SHMT along the MD simulations. (2) These results suggest that structures like compound **4** could be potential candidates for selective inhibitors of *Pf*SHMT. (3) Finally, the analysis of the residues present in the interaction surfaces of intermolecular contact in both enzymes revealed important residues in the actives sites not reported in the former studies by França et al. [12]. For *Hs*SHMT the residues Pro278, Ala358, Lys376 and Thr378 were involved in interactions with FFO and with compound **4**. For *Pf*SHMT the new residues were Phe135, Val141, Thr357 and Cys364. The studies of the potential interactions of these residues with new ligands could bring important improvements in the design of selective inhibitors for *Pf*SHMT.

Further studies are now on course in our lab in order to investigate the relevance of the new residues for selective inhibition and, also, to explore structures of 2,4-diaminopyrimidines analogues as potentially more efficient selective inhibitors of *Pf*SHMT.

Acknowledgements

We are grateful to IME, CNPq, FAPERJ and CAPES for funding this work.

References

[1] Available at http://portalweb02.saude.gov.br/portal/saude/visualizar_texto.cfm (accessed December 2008).
[2] Available at http://www.fiocruz.br/ccs/glossario/malaria.htm (accessed December 2008).
[3] I.S. Soares and M.M. Rodrigues, *Malaria vaccine: road-blocks and possible solutions*, Braz. J. Med. Biol. Res. 31 (1998), pp. 317–332.
[4] Available at http://www.who.int/malaria/malariaendemiccountries.html (accessed December 2008).
[5] *The World Health Organization Report*, WHO Publications, Geneva, 1997.
[6] W. Peters, *Drug resistance in malaria parasites of animals in man*, Adv. Parasitol. 41 (1998), pp. 1–62.
[7] S.J. Foote and A.F. Cowman, *The mode of action and the mechanism of resistance to antimalarial drugs*, Acta Trop. 56 (1994), pp. 157–171.
[8] P. Newton and N. White, *Malaria: new developments in treatment and prevention*, Annu. Rev. Med. 50 (1999), pp. 179–192.
[9] N.J. White and P.L. Olliaro, *Strategies for the prevention of antimalarial drug resistance: rationale for combination chemotherapy of malaria*, Parasitol. Today 12 (1996), pp. 399–401.

[10] R.T. Delfino, O.A. Santos Filho, and J.D. Figueroa-Villar, *Molecular modeling of wild-type and antifolate resistant mutant* Plasmodium falciparum *DHFR*, Biophys. Chem. 98 (2002), pp. 287–300.
[11] T.C.C. França, A.L.R. Medeiros, O.A. Santos Filho, E.C.P. Santos, and J.D. Figueroa-Villar, *A complete model of the* Plasmodium falciparum *bifunctional enzyme dihydrofolate reductase–thymidylate synthase. A model to design new antimalarials*, J. Braz. Chem. Soc. 15 (2004), pp. 450–454.
[12] T.C.C. França, P.G. Pascutti, T.C. Ramalho, and J.D. Figueroa-Villar, *A three-dimensional structure of* Plasmodium falciparum *serine hydroxymethyltransferase in complex with glycine and 5-formyl-tetrahydrofolate. Homology modeling and molecular dynamics*, Biophys. Chem. 115 (2005), pp. 1–10.
[13] T.C.C. França, A. Wilter, T.C. Ramalho, P.G. Pascutti, and J.D. Figueroa-Villar, *Molecular dynamics of the interaction of* Plasmodium falciparum *and human serine hydroxymethyltransferase with 5-formyl-6-hydrofolic acid analogues: design of new potential antimalarials*, J. Braz. Chem. Soc. 17 (2006), pp. 1383–1392.
[14] M.J. Frisch, G.W. Trucks, H.B. Schlegel, G.E. Scuseria, M.A. Robb, J.R. Cheeseman, V.G. Zakrewski, J.A. Montgomery, R.E. Stratman, J.C. Vurant, S. Dapprich, J.M. Millam, A.D. Daniels, K.N. Kudin, M.C. Strain, O. Farkas, J. Tomasi, V. Barone, M. Cossi, R. Cammi, B. Mennuci, C. Pomelli, C. Adamo, S. Clifford, J. Ochterski, G.A. Petersson, P.Y. Ayala, Q. Cui, K. Morokuma, D.K. Malick, A.D. Rabuch, K. Raghavachari, J.B. Foresman, J. Cioslowshi, J.V. Ortiz, B.B. Stefanov, G. Liu, A. Liashenko, P. Piskorz, I. Komaromi, R. Gomperts, R.L. Martin, D.J. Foz, T.M. AlLaham, C.Y. Peng, A. Nanayakkara, C. Gonzalez, M. Challacombe, P.M.W. Gill, B. Jonson, W. Chen, M.W. Wong, J.L. Andres, C. Gonzalez, M. Head-Gordon, E.S. Reploge, and J.A. Pople, *Gaussian 98, Revision A.11*, Gaussian, Inc., Pittsburgh, PA, 2001.
[15] A.W. Schuettelkopf and D.M.F. van Aalten, *PRODRG: a tool for high-throughput crystallography of protein–ligand complexes*, Acta Crystallogr., Sect. D: Biol. Crystallogr. 60 (2004), pp. 1355–1363.
[16] G.M. Morris, D.S. Goodsell, R.S. Halliday, R. Huey, W.E. Hart, R.K. Belew, and A.J. Olson, *Automated docking using a Lamarckian genetic algorithm and empirical binding free energy function*, J. Comput. Chem. 19 (1998), pp. 1639–1662.
[17] S.B. Renwick, K. Snell, and U. Baumann, *The crystal structure of human cytosolic serine hydroxymethyltransferase: a target for cancer chemotherapy*, Structure 6 (1998), pp. 1105–1116.
[18] E. Lindahl, B. Hess, and D. Van der Spoel, *GROMACS 3.0: a package for molecular simulation and trajectory analysis*, J. Mol. Model. 7 (2001), pp. 306–317.
[19] H.J.C. Berendsen, D. Van der Spoel, and R. Van Drunen, *GROMACS: a message-passing parallel molecular dynamics implementation*, Comput. Phys. Commun. 91 (1995), pp. 43–56.
[20] T.C.C. França, M.G. Santos, and J.D. Figueroa-Villar, *Malária: Aspectos Históricos e Quimioterapia*, Quim. Nova 31 (2008), pp. 1271–1278.
[21] R.T. Delfino, O.A. Santos Filho, and J.D. Figueroa-Villar, *Type 2 antifolates in the chemotherapy of falciparum malaria*, J. Braz. Chem. Soc. 13 (2002), pp. 727–741.
[22] E.F.F. da Cunha, T.C. Ramalho, E.R. Mala, and R.B. de Alencastro, *The search for new DHFR inhibitors: a review of patents*, Expert Opin. Ther. Pat. 15 (2005), pp. 967–986.
[23] J.N. Sarsdale, G. Kazanina, S. Radaev, V. Schirch, and T. Wright, *Crystal structure of rabbit cytosolic hydroxymethyltransferase at 2.8 Å resolution: mechanistic implications*, Biochemistry 38 (1999), pp. 8347–8358.
[24] L.P. Graham, *An Introduction to Medicinal Chemistry*, 2nd ed., Oxford University Press, Oxford, 2001.
[25] J.R. Pinheiro, M. Bitencourt, E.F.F. da Cunha, and T.C. Ramalho, *About docking and QSAR approaches novel anti-HIV cyclotriazadisulfonamide derivatives as modeled by ligand- and receptor-based approaches*, Bioorg. Med. Chem. 16(4) (2008), pp. 1683–1690.
[26] D. Josa, E.F.F. da Cunha, T.C. Ramalho, T.C.S. Souza, and M.S. Caetano, *Homology modeling of wild-type, D516V, and H526L* Mycobacterium tuberculosis *RNA polymerase and their molecular docking study with inhibitors*, J. Biomol. Struct. Dyn. 25(4) (2008), pp. 373–376.
[27] S.R. Dahmen, *Boltzmann's work in physics*, Rev. Bras. Ensino Fís. 28 (2006), pp. 281–295.
[28] L. Boltzmann, in *Wissenschaftliche Abhandlungen*, F. Hasenöhrl ed., Vol. I–III, Barth, Leipzig, reissued New York: Chelsea, 1969.
[29] J.L. Lebowitz, *Statistical mechanics: a selective review of two central issues*, Rev. Mod. Phys. 71 (1999), pp. S346–S357.
[30] S.B. Volchan, *A probabilidade na mecânica estatística clássica*, Rev. Bras. Ensino Fís. 28 (2006), pp. 313–318.
[31] T.C.C. França, M.R.M. Rocha, B.M. Reboredo, M.N. Rennó, L.W. Tinoco, and J.D. Figueroa-Villar, *Design of inhibitors for nucleoside hydrolase from* Leishmania donovani *using molecular dynamics studies*, J. Braz. Chem. Soc. 19 (2008), pp. 64–73.